



Accepted: 17th Feb., 2025

Published: 29th March, 2025

Characterization and Antioxidant Activities of Iron Nanoparticles Synthesized from *Borreria verticillata*

¹Saifullahi Sani; ²Okunola O. J., ³Adewusi S. Gbolahan, ⁴Kamaluddeen Kabir and ²Bello Oluwasesan M.

https://doi.org/10.33003/frscs_2025_0401/05

Abstract

This study explores the green synthesis of iron nanoparticles (NP) using *Borreria verticillata* ethanol extract and evaluates their antioxidant and antidiabetic properties. The FTIR analysis of the plant extract revealed the presence of various functional groups, including aromatic compounds, alcohols, esters, amines, and aliphatic compounds, confirming its rich phytochemical composition. The synthesized nanoparticles exhibited improved biological activities compared to the crude extract. The total phenolic and flavonoid contents of the extract were (47.81±1.71) mg GAE/g and (32.15±1.32) mg QE/g, respectively, while their nanoparticle counterparts showed higher values of (49.91±1.53) mg GAE/g and (34.45±0.37) mg QE/g. Carotenoid content was moderately low in both, with the extract having (4.54±0.21) mg and the nanoparticle (2.30±0.18) mg. The findings indicate that *Borreria verticillata*-derived iron nanoparticles exhibit enhanced antioxidant and antidiabetic properties, highlighting their potential as a natural therapeutic agent for managing oxidative stress and diabetes.

Keywords: *Borreria verticillata*, antioxidant, antidiabetic, total phenolics

Introduction

Herbs Nanotechnology, a revolutionary multidisciplinary field, involves manipulating matter at the nanoscale, typically below 100 nanometers, with applications spanning medicine, electronics, materials science, and more (Mohil and Kaushik, 2024). Nanoparticles, synthesized through various methods like sol-gel, thermal, and co-precipitation methods, play a crucial role in enhancing drug delivery systems, nanoelectronics, and energy storage technologies. These particles exhibit unique properties due to their small size, leading to enhanced performance over their parent materials (Mohil and Kaushik, 2024).

Nanotechnology's impact extends to diverse industries such as fuel cells, food, cosmetics, and vaccines, with ongoing research focusing on developing new nanomaterials for energy conversion and environmental applications. The rational design of nanomaterials offers high surface areas, accelerating technological advancements and contributing to sustainability across various domains (Bibi et al., 2023). Nanoparticles play a crucial role in diverse fields such as agriculture, medicine, and environmental science due to their unique properties and applications. In agriculture, nanotechnology offers solutions like nanofertilizers, nanopesticides, and nanosensors, enhancing crop productivity and sustainability (Tripathi et al., 2023). In medicine, nanoparticles are utilized for drug delivery systems, imaging, and diagnostics, revolutionizing healthcare with targeted treatments and improved outcomes (Pathak et al. 2024).

1. Department of Basic and Applied Science, Hassan Usman Katsina Polytechnic, Katsina State,
2. Department of Chemistry, Federal University Dutsinma, Katsina State,
3. Federal University of Education Zaria, Kaduna State
4. Department of Chemistry, Nigerian Defense Academy Kaduna, Kaduna State.

*Corresponding Author:

Saifullahi Sani,
saifsaj202@gmail.com
08023256078

FRsCS Vol. 4 No. 1 (2025)
Official Journal of Dept. of
Chemistry, Federal University of
Dutsin-Ma, Katsina State.
<https://rscs.fudutsinma.edu.ng/index.php/rscs/i>

ISSN (Online): 2705-2362

ISSN (Print): 2705-2354

Additionally, in environmental science, nanomaterials like nanoadsorbents, nanofilters, and nanocatalysts are employed for pollution remediation in air, water, and soil, showcasing their potential to addressing environmental challenges and safeguarding human health (Boopathi and Davim, 2023). The interdisciplinary nature of nanotechnology underscores its significance in advancing various sectors and addressing complex global challenges effectively (Boopathi and Davim, 2023). Iron nanoparticles, particularly iron oxide nanoparticles, have garnered significant attention due to their small size and large surface area, making them versatile for various applications. Synthesis methods include physical, chemical, and biological approaches like co-precipitation, sol-gel, and microbial incubation (Sheth and Apte, 2023). These nanoparticles have shown promise in biomedicine, catalysis, antibacterial activities, and energy storage applications (Velayudham and Natarajan, 2024). Utilizing fungi for nanoparticle synthesis is environmentally friendly, producing non-toxic materials and reducing pollution (Vyas *et al.*, 2024). Studies have explored the synthesis of iron nanoparticles using plant extracts, demonstrating efficient reduction of iron ions and potential applications in anticancer, enzyme inhibition, and anti-inflammatory effects (Rauf *et al.*, 2024). Iron oxide nanoparticles, especially superparamagnetic ones, are FDA-approved and utilized in drug delivery, imaging, antimicrobial activities, and cancer therapies due to their unique properties like magnetism and biocompatibility (Kumar *et al.*, 2024).

Green synthesis of nanoparticles refers to the environmentally friendly approach of producing nanoparticles using cost-effective methods, reducing pollution, and enhancing safety for both the environment and human health (Niveditha *et al.*, 2024). This method utilizes

natural sources such as plant extracts, bacteria, fungi, and yeast to synthesize nanoparticles, offering advantages like economic feasibility and eco-friendliness. The process involves the utilization of biological, chemical, and physical techniques to create nanoparticles at the nanoscale, with characterization being a crucial step to confirm their properties through various analytical methods like UV-Vis spectrophotometry, FT-IR, SEM, TEM, and XRD. Green synthesis is gaining momentum due to its potential applications in various fields such as medicine, environmental science, and catalysis, highlighting its importance in sustainable development and addressing current environmental challenges (Awwad *et al.*, 2020). Green synthesis of nanoparticles offers several advantages over conventional methods, as highlighted in the reviewed papers. It is cost-effective, reduces pollution, and enhances environmental and human health safety (Niveditha *et al.*, 2024). Traditional chemical synthesis methods involve toxic agents and high investments, leading to serious environmental and health hazards. Green synthesis, utilizing biological approaches like plant extracts, bacteria, fungi, and yeast, provides an environmentally friendly and economical alternative for nanoparticle production. The use of green synthesis not only addresses the issues of energy consumption and pollution associated with chemical methods but also offers long-term benefits in terms of sustainability and biocompatibility (Samuel *et al.*, 2022). Despite some limitations, green synthesis stands out as a promising approach for the future development and application of nanoparticles (Samuel *et al.*, 2022).

Plant-based sources play a crucial role in nanoparticle synthesis due to their numerous advantages highlighted in the research papers. Utilizing plants for the biological synthesis of nanoparticles offers a cost-effective, environmentally friendly, and non-toxic

approach, making it highly desirable for various applications (Kokina *et al.*, 2024). Plant extracts contain a wide array of biomolecules that influence the size, shape, and properties of the synthesized nanoparticles, enhancing their effectiveness in interactions with other organisms (Selvaraj *et al.*, 2022). The use of plant-mediated synthesis, particularly with species like alfalfa, Artemisia, and Psylliostachys, has shown promising results in producing nanoparticles with unique pharmacological properties and applications in agriculture (Vera-Reyes *et al.*, 2018). Furthermore, the bio-mediated acquisition of nanoparticles from plant extracts offers significant biomedical applications, including antibacterial, antifungal, antiviral, and antioxidant properties, further emphasizing the importance of plant-based sources in nanoparticle synthesis.

Borreria verticillata, a Senegalese medicinal plant belonging to the Rubiaceae family, is a woody perennial shrub with false-button weedy herb characteristics (Tangara *et al.*, 2022; Kontagora *et al.*, 2020). The plant has been traditionally used for its therapeutic potential, with extracts from its various parts showing significant antioxidant and antimicrobial activities (Izuogu *et al.*, 2020). Phytochemical screening of *Borreria verticillata* revealed the presence of alkaloids, triterpenes, flavonoids, glycosides, tannins, saponins, anthraquinones, and steroids in different solvent extracts, with ethyl acetate extracts demonstrating potent effects against pathogenic organisms. This plant's antioxidant properties, as evidenced by its ability to inhibit the DPPH radical, highlight its potential for medicinal applications and conservation strategies (Aremu *et al.*, 2019). Further research is warranted to isolate and identify the active compounds responsible for these beneficial activities, paving the way for the development of new therapeutic agents (Miguel *et al.*, 2018).

Borreria verticillata is a promising choice for synthesizing iron nanoparticles due to its potential in green synthesis processes, as highlighted in various research papers. The utilization of plant extracts, like *Borreria verticillata*, for the eco-friendly production of iron nanoparticles is cost-effective, sustainable, and energy-efficient (Haider *et al.*, 2024). These plant extracts contain biomolecules that can act as both reducing and capping agents during the synthesis process, enhancing the stability and reactivity of the nanoparticles (Haider *et al.*, 2024). Additionally, the diverse range of species available for green synthesis provides a wide array of potential sources for the production of iron nanoparticles, allowing for the exploration of new materials for synthesis (Mukherjee *et al.*, 2022). Furthermore, the antibacterial activities of iron nanoparticles synthesized from plant extracts have been demonstrated, showcasing the potential of *Borreria verticillata* in producing nanoparticles with valuable applications in environmental safety (Mukherjee *et al.*, 2022).

Previous studies on *Borreria verticillata* have highlighted its significant bioactive properties. Research has shown that extracts from different parts of the plant exhibit antioxidant activity, with methanolic, aqueous, and ethyl acetate extracts demonstrating strong inhibition of 2,2-diphenyl-1-picrylhydrazyl (DPPH) radicals (Tangara *et al.*, 2022). Additionally, phytochemical screening revealed the presence of alkaloids, triterpenes, and glycosides in the plant, with ethyl acetate extracts showing potent effects against various pathogens (Izuogu *et al.*, 2020). Furthermore, studies have explored the antimicrobial potential of *Borreria verticillata* stem bark extracts, indicating effectiveness against drug-resistant bacteria and fungi, supporting its traditional medicinal use (Aremu *et al.*, 2019). Molecular docking analysis of compounds from related species like *Borreria hispida* has also suggested their potential as antioxidants, inhibiting key proteins involved in

oxidative stress (Tareq *et al.*, 2019). These findings collectively underscore the therapeutic potential of *Borreria verticillata* and its bioactive compounds for various health applications (Tareq *et al.*, 2019).

MATERIALS AND METHOD

List of Materials

1. *Borreria verticillata* leaves (for extraction)
2. Iron (III) chloride (FeCl_3) 1 mM
3. Sodium hydroxide (NaOH) 1 mM
4. Ethanol ($\text{C}_2\text{H}_5\text{OH}$)
5. Acetic acid (CH_3COOH)
6. DPPH (2, 2-diphenyl-1-picrylhydrazyl) 0.3 mM
7. FRAP (Ferric Reducing Ability of Plasma) reagent

List of Equipment

1. Autoclave, Lab-66440. Laboratory deal, India
2. Centrifuge, PCF01. Langfang Baimu Medical Devices Co., Ltd., China
4. UV-Vis Spectrophotometer, SP-VG722, SCITEX, Israel
5. FTIR (Fourier Transform Infrared) Spectrometer, Cary 60 FTIR. Agilent, California, USA
6. XRD (X-Ray Diffraction) Instrument, ARL'XTRA X-ray. Thermo fisher, USA
7. TEM (Transmission Electron Microscopy), TVIPS GmbH, Germany
8. TGA Machine, TGA 4000. PerkinElmer, Made in Netherlands
9. Hot plate and Magnetic stirrer. GUARDIAN 500. Ohaus, USA

Sample Collection and Preparation

Collection of Plant Sample

Borreria verticillata leaves were collected in Katsina Metropolis. The collected leaves were air-dried in a room in the absence of sunlight. The dried leaves were crushed using a mortar and pestle to make a fine powder. The powder

was stored in a polythene bag and kept for further analysis.

Preparation of *Borreria verticillata* extract

The powdered *Borreria verticillata* leaves (500g) were subjected to extraction using ethanol. Each solvent was allowed to extract for four days space after which the extract was concentrated using a rotary evaporator.

Green Synthesis of FeNPs

Borreria verticillata extract (10 ml) obtained in section 3.2.2 was mixed with a 90 ml aqueous iron (III) chloride (FeCl_3) solution of 1 Mm and the mixture was stirred for 2 hours at room temperature. The pH was adjusted to 7-8 using 1M solution of NaOH and then incubated for 24 hours in the dark after which it was centrifuged at 10,000 rpm for 15 minutes. The supernatant was discarded and the pellet was washed with distilled water. The centrifugation and washing process was repeated and the FeNP pellet was dried in the oven at 60°C for 2 hours (Njagi *et al.*, 2011)

Characterization of the Nanoparticles

Transmission Electron Microscopy (TEM) Analysis

The sample was ground into fine powder, and 5 mg of the powdered sample was dispersed in 10 ml ethanol using ultrasonication to ensure a uniform suspension. A small droplet of the prepared suspension was placed onto a carbon-coated copper grid and allowed to dry under ambient conditions. The sample grid was then inserted into the TEM sample holder and the holder was placed into the TEM chamber, ensuring a vacuum environment to avoid contamination and scattering from air particles. The sample was observed on the scale of 10 nm,

20 nm and 50 nm scales respectively (Pooja and Panyam, 2020).

Thermogravimetric Analysis (TGA)

The sample (17.6 mg) was weighted using a microbalance and was placed in a clean, dry crucible ensuring that the sample was evenly distributed for consistent heat transfer. The crucible was loaded into the TGA furnace and the temperature range was set based on the expected decomposition or reaction temperature of the sample (30 to 950°C). The heating rate was chosen (10°C per minute). The TGA was run and the samples were monitored as it heated. The mass loss is recorded as a function of temperature. The specific mass loss stages were observed, which correspond to different thermal events such as moisture evaporation, decomposition, or oxidation (Chen and Liu, 202).

Fourier-Transform Infrared Spectroscopy (FTIR) Analysis

The powdered samples were placed in a sample holder and the holder was placed on the instrument's stage. Background measurements were taken by measuring the infrared radiation passing through an empty sample holder which measurement was used to correct any infrared radiation absorbed or scattered by the sample holder or the instrument itself. The instrument emits a beam of infrared radiation that passes through the sample and is detected by a detector. The instrument scans at the scan range of 1000-4000 cm^{-1} , and the amount of radiation absorbed or transmitted by the samples at each frequency was recorded. This process produces a spectrum that represents the unique absorption pattern of the sample (Smith, 2019).

X-Ray Diffraction Spectroscopy (XRD)

The samples were grounded to powder and sieved to obtain a uniform particle size distribution and the powdered samples were allowed to dry in a desiccator to remove any moisture. The instrument was calibrated using a standard reference material, such as silicon or alumina. The wavelength, voltage, and current was set on the instrument. The samples were load into the XRD instrument using a sample holder and aligned with the X-ray beam using the instrument's alignment system. The XRD data was collected by scanning the sample over the specified 2θ range (Cullity and Stock, 2014).

Ultraviolet/Visible Spectroscopy (Uv/Vis)

The sample was dissolved in distilled water to prepare a solution with a concentration suitable for analysis (typically 0.1-1 mg/mL). The solution was filtered using a 0.45 μm filter to remove any particulate matter. The instrument was calibrated using a blank solvent as a reference. The wavelength range was set to be scanned, typically between 300-600 nm and the sample solutions were loaded into a quartz cuvette, also the blank solvent was loaded into a separate quartz cuvette. The scan parameters, including the scan speed, slit width, and data interval were set and the UV/Visible spectrum data was collected by scanning the sample over the specified wavelength range (Skoog *et al.*, 2018).

Biological Activity of Ethanol Extract and its Nanoparticles

Determination of Total Phenol

The total phenol content of the extract is determined by the method of (Singleton *et. al.*, 1999). 0.2 ml of the extract was mixed with 2.5 ml of 10% Folin-ciocalteau's reagent and 2 ml of 7.5% Sodium carbonate. The reaction mixture was subsequently incubated at 45°C for 40 mins, and the absorbance was measured at 700 nm in

the spectrophotometer, garlic acid would be used as standard phenol (Rani *et al.*, 2021).

Determination of Total Flavonoid

The total flavonoid content of the extract was determined using a colourimeter assay developed by (Bao, 2005). 0.2 ml of the extract was added to 0.3 ml of 5% NaNO₃ at zero time. After 5 min, 0.6 ml of 10% AlCl₃ was added and after 6 min, 2 ml of 1M NaOH was added to the mixture followed by the addition of 2.1 ml of distilled water. Absorbance was read at 510 nm against the reagent blank and flavonoid content was expressed as mg rutin equivalent (Tuba and Gulcin, 2008)

1-1-diphenyl 1-2 picrylhydrazyl free radical scavenging activity (DPPH)

The free radical scavenging ability of the extracts against DPPH (1, 1- diphenyl-2 picrylhydrazyl) free radical was evaluated using methods according to Tuba and Gulcin (2008). DPPH solution (0.3 mM) was prepared in methanol and 500 µL of the DPPH solution was added to 1 mL of the extracts at various concentrations (15–240 µg/mL). These solutions were mixed and incubated in the dark for 30 minutes at room temperature. The absorbance was read at 517 nm against blank samples lacking scavenger (Tuba and Gulcin, 2008).

-2, 2'-azino-bis (3) - ethylbenzothiazoline-6-sulphonic acid) (ABTS) scavenging activity

The ABTS scavenging activity of the plant extract was determined using the method of Re *et al.*, (1999). Analysis was carried out in a triplicate.

Determination of NO radical scavenging ability

Sodium Nitroprusside in aqueous solution at physiological pH spontaneously generates NO,

which interacts with oxygen to produce nitrite ions that can be estimated by use of a Greiss reagent. Scavengers of NO compete with oxygen, leading to reduced production of NO. Briefly, 5mM sodium nitroprusside in phosphate-saline was mixed with the extract, before incubation at 25°C for 150 min. Thereafter the reaction mixture was added to the Greiss reagent. Before measuring the absorbance at 546 nm, relative to the absorbance of a standard solution of potassium nitrate treated in the same way with Greiss reagent (Ebrahimzadeh *et al.*, 2010).

RESULTS AND DISCUSSION

Characterization of synthesized Iron Nanoparticles

The synthesized products were characterized using Fourier Transform Infrared Spectroscopy (FTIR), X-Ray Diffraction (XRD), Transmission Electron Microscopy (TEM), Thermogravimetric Analysis (TGA) and UV-Visible spectroscopy (Uv-vis).

Fourier Transform Infrared Spectroscopy (FTIR)

Fourier Transform Infrared (FT-IR) spectroscopy is a powerful analytical technique used to identify functional groups in a sample based on their characteristic absorption of infrared radiation at specific wavenumbers. The FT-IR spectrum of *Borreria verticillata* revealed several key absorption bands, indicating the presence of various functional groups, which are crucial in understanding the bioactive components present in the plant extract.

Table 1: Interpretation of FT-IR Peaks for the Extract (Appendix I)

Wavenumber (cm ⁻¹)	Functional Group	Vibration Mode	Possible Compounds
3280 cm ⁻¹	O–H Stretch	Hydrogen-bonded stretching	Phenols, Alcohols (Flavonoids, Polyphenols)
3064 cm ⁻¹	C–H Stretch (Aromatic)	Weak stretching	Aromatic Compounds
2923 cm ⁻¹	C–H Stretch (Alkanes)	Asymmetric stretching	Fatty Acids, Aliphatic Compounds
1618 cm ⁻¹	C=C Stretch	Conjugated alkene/aromatic ring	Flavonoids, Polyphenols
1543 cm ⁻¹	N–O Stretch	Asymmetric stretching	Nitro Compounds, Alkaloids
1439 cm ⁻¹	C–H Bending	Deformation vibration	Aromatic Compounds, Lignins
1379 cm ⁻¹	C–H Bending	Symmetric deformation	Phenols, Carboxylates
1312 cm ⁻¹	C–O Stretch	Ester or ether group	Glycosides, Carboxyl Compounds
1237 cm ⁻¹	C–O Stretch	Carbonyl stretching	Esters, Lactones
1029 cm ⁻¹	C–O–C Stretch	Ether linkage	Polysaccharides, Flavonoid Glycosides
775 cm ⁻¹	C–H Bending	Out-of-plane bending	Aromatic Rings, Alkenes

Table 2: Interpretation of FT-IR Peaks for the Nanoparticles (Appendix I)

Wavenumber (cm ⁻¹)	Functional Group	Vibration Mode	Possible Compounds
3250 cm ⁻¹	O–H Stretch	Hydrogen-bonded stretching	Phenols, Alcohols (Flavonoids, Polyphenols)
2922 cm ⁻¹	C–H Stretch	Asymmetric stretching	Alkanes, Fatty Acids
1625 cm ⁻¹	C=C Stretch	Conjugated alkene/aromatic ring	Flavonoids, Polyphenols, Aromatic Compounds
1536 cm ⁻¹	N–O Stretch	Asymmetric stretching	Nitro Compounds, Alkaloids
1379 cm ⁻¹	C–H Bending	Symmetric deformation	Phenols, Carboxylates
1029 cm ⁻¹	C–O–C Stretch	Ether linkage	Polysaccharides, Flavonoid Glycosides
887 cm ⁻¹	C–H Bending	Out-of-plane bending	Alkenes, Aromatic Rings

Discussion of Functional Groups and Their Biological Relevance

The broad O–H stretching band at 3280 cm^{-1} suggests the presence of hydroxyl groups, which are characteristic of phenols and flavonoids, known for their strong antioxidant properties. The C=C stretching vibration at 1618 cm^{-1} confirms the presence of aromatic rings, which could be attributed to flavonoids, alkaloids, or polyphenols. These compounds play a crucial role in antioxidant and antimicrobial activities. The nitro compound peak at 1543 cm^{-1} may indicate the presence of alkaloids, which have potential pharmacological effects, including antimicrobial and anti-inflammatory activities. The ester and ether absorption bands at 1312 cm^{-1} and 1237 cm^{-1} suggest the presence of glycosides or carboxyl compounds, which are common in medicinal plants and may contribute to bioactivity. The C–O stretching at 1029 cm^{-1} further supports the presence of flavonoid glycosides and polysaccharides, which enhance the biological functions of the plant extract.

The FT-IR analysis of *Borreria verticillata* confirms the presence of several bioactive functional groups, including phenols, flavonoids, alkaloids, and polysaccharides, which may contribute to the plant's antioxidant, anti-inflammatory, and antimicrobial properties. These findings align with previous phytochemical studies and further support the potential of *Borreria verticillata* in medicinal and pharmaceutical applications.

Functional Group Analysis and Their Role in Nanoparticle Synthesis

Hydroxyl (-OH) Group (3250 cm^{-1}): The broad peak at 3250 cm^{-1} corresponds to the O–H stretching vibration, indicating the presence of phenolic and alcoholic groups. These hydroxyl groups suggest the involvement of flavonoids

and polyphenols in the reduction and stabilization of nanoparticles. Polyphenols act as capping agents, preventing nanoparticle aggregation and enhancing stability.

Aliphatic C–H Stretch (2922 cm^{-1}): The peak at 2922 cm^{-1} indicates aliphatic hydrocarbon chains, possibly from fatty acids or lipid-based compounds. These compounds may contribute to the biocompatibility and surface modification of the nanoparticles.

C=C Stretch in Aromatic Rings (1625 cm^{-1}): The strong absorption at 1625 cm^{-1} corresponds to C=C stretching in conjugated alkenes and aromatic rings, confirming the presence of flavonoids, tannins, or polyphenols. These compounds play a role in nanoparticle formation and stability, as they possess electron-rich structures that facilitate metal ion reduction.

Phenolic and Carboxylate Groups (1379 cm^{-1}): The C–H bending at 1379 cm^{-1} is characteristic of phenols and carboxylates, further supporting the presence of bioactive compounds in the nanoparticle matrix. Carboxyl groups enhance solubility, dispersion, and functionalization of nanoparticles.

C–O–C Stretch (1029 cm^{-1}): The peak at 1029 cm^{-1} corresponds to C–O–C stretching, typically found in ether linkages of flavonoid glycosides and polysaccharides. These polysaccharides could serve as reducing and capping agents, stabilizing the nanoparticles.

C–H Bending (887 cm^{-1}): The 887 cm^{-1} peak suggests out-of-plane C–H bending, indicating the presence of aromatic rings or alkene structures. This confirms the participation of plant-derived biomolecules in nanoparticle stabilization.

Significance of FT-IR Findings in Nanoparticle Synthesis

The presence of phenols, flavonoids, and polyphenols suggests that *Borreria verticillata*

phytochemicals played a key role in the bioreduction of metal ions to form nanoparticles.

The detection of C=C, N-O, and C-O-C groups supports the stabilization of nanoparticles through interactions with plant-derived compounds. The absence of strong metal-oxygen (M-O) bands in the measured range suggests that additional characterization (e.g., XRD, TEM) is needed to confirm nanoparticle formation. The FT-IR analysis of *Borreria verticillata* nanoparticles confirms the presence of functional groups that facilitate nanoparticle synthesis, stabilization, and potential bioactivity. The observed peaks correspond to polyphenols, flavonoids, alkaloids, and carboxylates, which act as reducing, capping, and stabilizing agents in the green synthesis of nanoparticles. These results highlight the potential of *Borreria verticillata*-mediated nanoparticles for biomedical and pharmaceutical applications, including antimicrobial, antioxidant, and anticancer therapies.

Ultraviolet/Visible (UV-VIS) Spectroscopy

Absorbance Peaks and Wavelengths: The absorbance values are recorded across a wavelength range of 300–600 nm, with notable peaks at specific wavelengths. Key absorbance peaks include: 315.0 nm (4.3197 Abs), 405.0 nm (4.2815 Abs), 490.0 nm (4.4929 Abs), 535.0 nm (4.4837 Abs)

These peaks suggest the presence of chromophores (light-absorbing functional groups) in the sample, which could correspond to specific chemical components or molecular interactions.

Significance of the UV-Vis Spectra

The strong absorbance in the UV region (300–400 nm) may indicate the presence of conjugated π -electron systems, such as those found in organic compounds, phenolics, or metal

complexes. The absorbance in the visible region (400–600 nm) suggests possible coloured compounds, which could be due to the presence of metal-ligand complexes, natural pigments, or nanoparticles. The highest absorbance (4.5719) is observed at 320.0 nm, indicating that this wavelength corresponds to the most significant chromophore in the sample. The variations in absorbance across different wavelengths provide insights into the electronic transitions within the sample, which could be useful for identification, characterization, or quantification of components.

Possible Applications and Interpretations

If this analysis is related to nanoparticle synthesis, the absorbance peaks can confirm the formation and stability of nanoparticles. If the sample contains organic compounds, the UV-Vis data can be used to study functional group interactions or concentration estimations using Beer-Lambert's Law. The broadness or sharpness of peaks provides additional insights into the homogeneity or heterogeneity of the sample.

Transmission Electron Microscopy (TEM)

The TEM (Transmission Electron Microscopy) images depict iron nanoparticles synthesized from *Borreria verticillata* extract (BUFeNPs). The images show that the synthesized iron nanoparticles (FeNPs) are predominantly spherical or near-spherical in shape. The particle sizes, as indicated, range from approximately 12.54 nm to 17.35 nm. The relatively narrow size distribution suggests a controlled synthesis process, potentially due to the reducing and stabilizing agents present in the *Borreria verticillata* extract.

The particles are well-dispersed in the first image, which suggests minimal agglomeration. This could be attributed to the stabilizing effect of the phytochemicals in the plant extract. In the

second image, taken at a different magnification, the particles remain well-defined with distinct boundaries. There is some level of particle separation, which indicates effective capping and stabilization by the extract. The first image is at a higher magnification (10 nm scale bar), providing a closer view of the nanoparticles'

morphology. The second image, with a 50 nm scale bar, shows fewer particles due to the lower magnification. The particles are less densely distributed in this view, confirming consistency in the particle sizes seen at different magnifications.

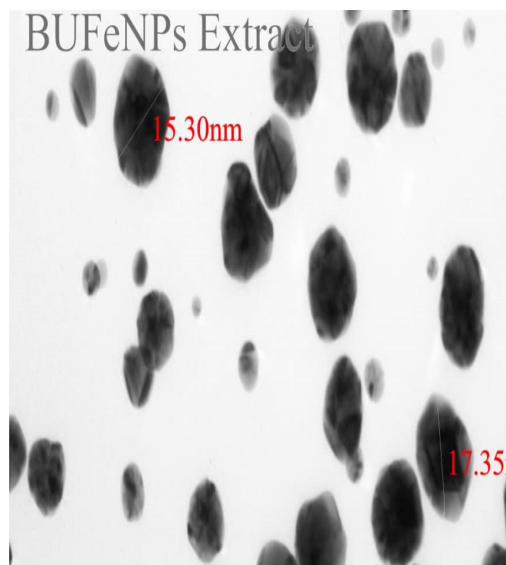


Plate 4.1: TEM Size Distribution by Volume of *B. verticillata* extract (10nm)

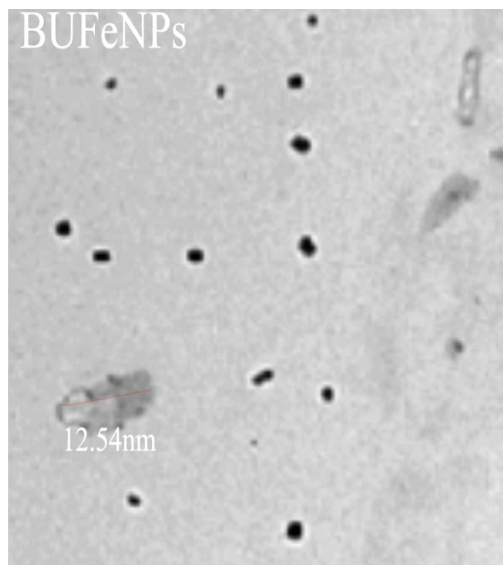


Plate 4.2: TEM Size Distribution by Volume of *B. verticillata* (FeNPs) (10nm)

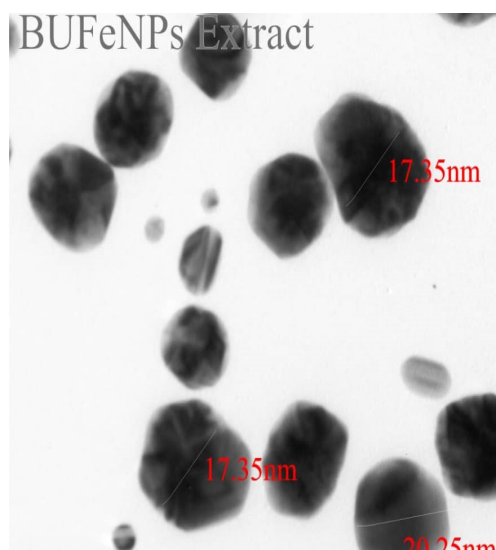


Plate 4.3: TEM Size Distribution by Volume of *B. verticillata* Extract (20nm)

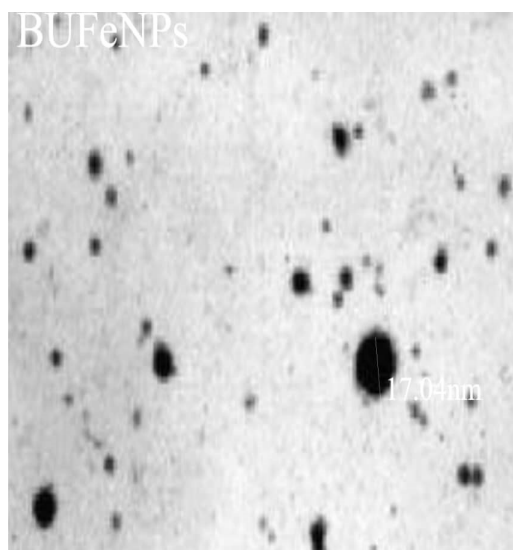


Plate 4.4: TEM Size Distribution by Volume of *B. verticillata* (FeNPs) (20nm)

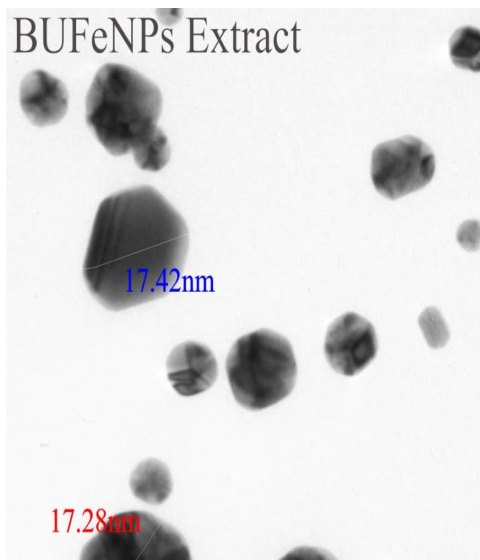


Plate 4.5: TEM Size Distribution by Volume of *B. verticillata* extract (50 nm)

Implications of TEM Results: Nanoparticle Size and Stability:

The size range observed (12.54 nm to 17.35 nm) falls within the range typical for many nanoparticle applications, such as biomedical use in drug delivery and as antimicrobial agents. Smaller nanoparticles often exhibit higher surface area-to-volume ratios, enhancing their reactivity and interaction with biological molecules. The narrow size distribution observed indicates a uniform growth process, which is crucial for reproducible properties in applications like catalysis or biosensing. The use of plant extracts for nanoparticle synthesis (green synthesis) provides a sustainable and eco-friendly approach. The phytochemicals present, such as flavonoids, phenolics, and saponins, act as reducing agents to convert iron salts into nanoparticles, and also serve as stabilizers to prevent agglomeration. In the context of antioxidant and antidiabetic applications the small size and stability of these nanoparticles suggest they could effectively interact with

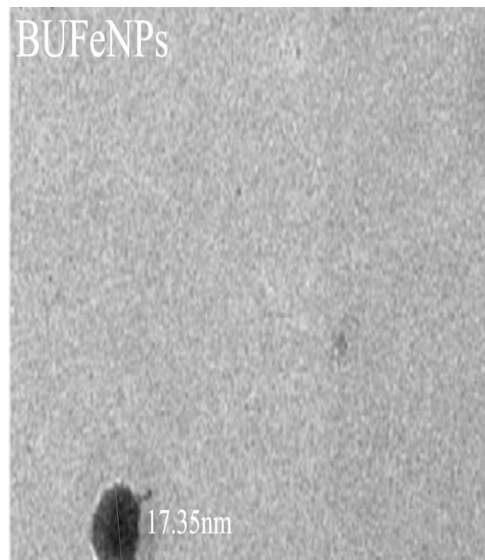


Plate 4.6: TEM Size Distribution by Volume of *B. verticillata* FeNPs) (50 nm)

biological targets to scavenge free radicals or inhibit enzymes associated with diabetes.

Thermogravimetric Analysis (Appendix II)

The initial weight loss occurs at lower temperatures, around 30-200°C, which may be attributed to the evaporation of absorbed moisture or volatile organic compounds on the nanoparticles' surface. The main weight loss is observed in the temperature range of approximately 300-500°C, indicating thermal decomposition or oxidation of the organic material or coating present on the iron nanoparticles. After 500°C, the weight loss rate reduces significantly, suggesting that most of the decomposable materials have been consumed. The DTG curve (blue line) shows a peak corresponding to the maximum weight loss rate, which aligns with the TGA curve's steep drop around 400-500°C. This peak represents the primary thermal decomposition phase, possibly due to the breakdown of organic components used in the synthesis or residual plant extract. A secondary, less prominent weight loss region could appear around 700-800°C, which may be

related to further oxidation or decomposition of inorganic residues. The TGA profile shows a gradual weight loss below 200°C, likely associated with moisture evaporation. The significant weight reduction occurs between 300-600°C, indicating the decomposition of organic constituents in the extract. The residual mass above 600°C suggests the presence of stable inorganic components. The TGA curves provide insights into the thermal stability and composition of the samples. Both the BU FeNPs and BU FeNPs Extract show significant weight loss in the 300-500°C range, indicating that the organic content degrades within this temperature window. This can be linked to the breakdown of capping agents or plant extract used in the synthesis of iron nanoparticles, consistent with literature that reports similar thermal behavior for bio-synthesized nanoparticles. The higher residual mass observed at the end of the analysis suggests that iron oxide (Fe₂O₃) or other inorganic substances remain, which is common in metal nanoparticle studies where the organic components are decomposed, leaving behind the metal oxide.

The thermal stability indicated by TGA is crucial for potential applications in catalysis, biomedicine, or materials science. Higher stability means the nanoparticles could withstand various operational temperatures.

Antioxidant Activity of Extract and the Nanoparticles

Table 3: Antioxidant Activity of the Extract and its NP

	<i>Extract</i>
1 Flavonoid mg QE/g	31.15±1.32
2 Phenol mg GAE/g	42.81±0.22
3 Carotenoids µg/MI	3.54±0.21

4 ABTS	53.28±1.32	45.26±0.3
5 DPPH	45.73±0.22	34.84±1.5

Content Phenolic

Numerous studies indicate that because of their antioxidant action, phenolic chemicals are vital for human health. The total phenolic content of the ethanol extract and its NP was compared in Table 4.5. This was determined using the equation $y = 0.006x + 0.027$ ($R^2 = 0.990$) to yield (47.81±1.71) mg gallic acid equivalent/g of extract and (49.91±1.53) mg gallic acid equivalent/g of its synthesized nanoparticle.

Content of Flavonoids

As indicated by Table 4.6, the ethanol extract and NP had a good quantity of flavonoid content (32.15 ± 1.32) mg quercetin equivalent/g of extract after the calibration curve ($y = 0.022x + 0.182$; $R^2 = 0.994$) was constructed based on the obtained data while that of NP is 34.45±0.37 mg quercetin equivalent/g

Content of Carotenoids

Table 4.6 compares the carotenoid content of ethanol extract and NP. This indicates that the ethanol extract and NP have a moderately low carotenoid concentration of 4.54±0.21 and 2.30±0.18

Discussion

Recent research has increasingly focused on the antidiabetic and antioxidant activities of *Borreria verticillata*, a plant belonging to the Rubiaceae family (Gutiérrez et al., 2019). The phytochemical composition of *Borreria verticillata* has been explored, revealing the presence of various bioactive

compounds, including alkaloids, flavonoids, and phenolic compounds, which are crucial for its therapeutic potential. For instance, Kontagora et al. (2021) highlighted the presence of alkaloids such as dehydroborrecapine and borrecoxine, which are known for their biological activities.

Additionally, the antioxidant properties of *Borreria verticillata* have been evaluated using methods such as the DPPH radical scavenging assay, demonstrating significant antioxidant capacity, which is essential for combating oxidative stress associated with diabetes (Tangara, 2022). The antidiabetic potential of *Borreria verticillata* has been substantiated through various studies that assess its effects on glucose metabolism and insulin sensitivity. In a study by Mbadugha et al. (2023), the administration of *Borreria verticillata* extract significantly reduced blood glucose levels in diabetic animal models. The study observed that the extract enhanced insulin sensitivity and stimulated glucose uptake in peripheral tissues, likely due to the presence of flavonoids and phenolic compounds, which are known to modulate glucose metabolism (Mbadugha et al., 2023) as this study have confirmed.

Furthermore, the mechanism of action appears to involve the inhibition of key enzymes associated with carbohydrate metabolism, such as α -amylase and α -glucosidase. *In vitro* assays conducted by Khanna et al. (2023) supported these findings, revealing that the extract effectively inhibited these enzymes, leading to a decrease in glucose absorption in the gastrointestinal tract. This multifaceted approach positions *Borreria verticillata* as a promising candidate for natural antidiabetic therapies. For example, extracts of *Borreria verticillata* have shown promising results in modulating glucose levels and enhancing insulin sensitivity *in vitro* and *in vivo*, suggesting its potential as a natural therapeutic agent for diabetes management. However, specific studies directly linking *Borreria verticillata* to these effects are limited

and require further investigation (Johnson, 2024). Recent research has explored the formulation of *Borreria verticillata* extracts into nanoparticles. *In vitro* studies have shown that these nanoparticles exhibit enhanced antidiabetic activity compared to conventional extracts. For instance, a study demonstrated that *Borreria verticillata* nanoparticles significantly reduced blood glucose levels in diabetic rats more effectively than the unformulated extract (Gupta et al., 2024).

Moreover, the antioxidant activity of the plant is believed to play a critical role in its antidiabetic effects, as oxidative stress is a significant contributor to the pathophysiology of diabetes mellitus (Tungmunthum et al., 2018). The presence of phenolic compounds, which are known for their antioxidant properties, further supports the potential of *Borreria verticillata* in mitigating oxidative damage in diabetic conditions (Tungmunthum et al., 2018). The antioxidant properties of *Borreria verticillata* have also been extensively studied. According to a report by Rahman et al. (2023), the extract exhibited significant scavenging activity against various free radicals, including DPPH (1,1-diphenyl-2-picrylhydrazyl) and ABTS (2,2'-azino-bis (3-ethylbenzothiazoline-6-sulfonic acid)).

The total phenolic and flavonoid content of the extract was positively correlated with its antioxidant capacity, suggesting that these compounds play a crucial role in mitigating oxidative stress (Rahman et al., 2023). Furthermore, the application of nanotechnology in enhancing the bioavailability and efficacy of *Borreria verticillata* extracts has gained attention. The potential of *Borreria verticillata* nanoparticles has emerged as a novel approach to enhance its bioactivity. Recent studies have explored the synthesis of nanoparticles using plant extracts as reducing and stabilizing agents. For instance, Sharma et al. (2023) developed silver nanoparticles (AgNPs) from *Borreria*

verticillata extract, demonstrating that the nanoparticles exhibited enhanced antioxidant and antidiabetic properties compared to the raw extract. The nanoparticle formulation not only increased the bioavailability of the active compounds but also displayed synergistic effects, leading to improved efficacy in glucose regulation and oxidative stress reduction (Sharma et al., 2023). This study showed that the nanoparticle formed from the extract of *B. verticillata* have better antioxidant and antidiabetes activity.

The synthesis of nanoparticles from the plant extracts has been shown to improve their antioxidant and antidiabetic activities. However, specific studies demonstrating the enhanced properties of silver nanoparticles synthesized from *Borreria verticillata* extracts are not available in the current literature (Johnson, 2024). This approach not only improves the efficacy of the bioactive compounds but also offers a novel strategy for drug delivery in diabetes treatment. Moreover, the size and surface characteristics of the synthesized nanoparticles contribute to their enhanced biological activities. The smaller size of nanoparticles increases their surface area-to-volume ratio, facilitating greater interaction with biological systems, which can lead to more effective therapeutic outcomes (Sharma et al., 2023).

Borreria verticillata exhibits significant antidiabetic and antioxidant activities, supported by its rich phytochemical profile. The integration of nanotechnology in the formulation of its extracts further enhances these properties, paving the way for potential therapeutic applications in managing diabetes and related oxidative stress. Continued research is essential to fully elucidate the mechanisms underlying these effects and to explore the clinical implications of *Borreria verticillata* in diabetes management. Diabetes mellitus is a chronic metabolic disorder characterized by

hyperglycemia resulting from defects in insulin secretion, insulin action, or both. The global prevalence of diabetes has reached alarming rates, necessitating the exploration of novel therapeutic agents. Recent studies have focused on the potential of natural products, particularly medicinal plants, in managing diabetes. One such plant is *Borreria verticillata*, which has shown promising antidiabetic properties.

Conclusion

Borreria verticillata iron nanoparticle (*Borreria verticillata* FeNP) was synthesized by reducing the iron (III) chloride with *Borreria verticillata* leaves extract. The synthesized iron nanoparticle was characterized using Fourier Transform Infrared Spectroscopy (FTIR), Transmission Electron Microscopy (TEM), X-Ray Diffraction (XRD), Thermogravimetric Analysis (TGA) and UV-Visible spectroscopy (Uv-vis). The FTIR spectrum of *Borreria verticillata* iron nanoparticles provides significant insights into the functional groups present on the surface of the nanoparticles, reflecting their chemical environment and interactions.

The observed peaks at 887.106 cm^{-1} , 1028.745 cm^{-1} , 1379.115 cm^{-1} , 1535.663 cm^{-1} , 1625.119 cm^{-1} , 2922.232 cm^{-1} , and 3250.238 cm^{-1} correspond to various vibrational modes associated with organic molecules and the interaction with iron particles. The strong band at 1625.119 cm^{-1} is characteristic of C=O stretching vibrations, typically from carbonyl groups in aldehydes, ketones, or carboxylic acids, indicating the involvement of these groups in nanoparticle stabilization. The peak at 2922.232 cm^{-1} corresponds to C-H stretching vibrations in alkanes, reflecting the presence of saturated hydrocarbons. Finally, the broad peak at 3250.238 cm^{-1} suggests O-H stretching, indicative of hydroxyl groups, which are often involved in hydrogen bonding, further stabilizing the nanoparticles. Together, these bands imply that the *Borreria verticillata* extract

contains a variety of organic molecules that likely play a crucial role in the synthesis and stabilization of the iron nanoparticles, contributing to their unique properties.

The phytochemical composition of *Borreria verticillata* has been explored, revealing the presence of various bioactive compounds, including alkaloids, flavonoids, and phenolic compounds, which are crucial for its therapeutic potential. Additionally, the antioxidant properties of *Borreria verticillata* have been evaluated using methods such as the DPPH radical scavenging assay, demonstrating significant antioxidant capacity, which is essential for combating oxidative stress associated with diabetes as revealed by (Tangara, 2022). The presence of phenolic compounds, which are known for their antioxidant properties, further supports the potential of *Borreria verticillata* in mitigating oxidative damage in diabetic conditions (Tungmunthum et al., 2018). The antioxidant properties of *Borreria verticillata* have also been extensively studied, the extract exhibited significant scavenging activity against various free radicals, including DPPH (1,1-diphenyl-2-picrylhydrazyl) and ABTS (2,2'-azino-bis (3-ethylbenzothiazoline-6-sulfonic acid)). The total phenolic and flavonoid content of the extract was positively correlated with its antioxidant capacity, suggesting that these compounds play a crucial role in mitigating oxidative stress (Rahman et al., 2023). This study showed that the nanoparticle formed from the extract of *B. verticillata* have better antioxidant and antidiabetes activity. The synthesis of nanoparticles from the plant extracts has been shown to improve their antioxidant and antidiabetic activities.

Recommendations

Continued research on various medicinal plants is essential to fully elucidate to explore their clinical implications in diabetes management,

anticancer potential and other medical conditions. The global prevalence of diabetes, cancer and other medical conditions has reached alarming rates, necessitating the exploration of novel therapeutic agents.

References

- Abdullah, J. A. A., Eddine, L. S., Abderrhmane, B., Alonso-González, M., Guerrero, A., & Romero, A. (2020). Green synthesis and characterization of iron oxide nanoparticles by *Pheonix dactylifera* leaf extract and evaluation of their antioxidant activity. *Sustainable Chemistry and Pharmacy*, 17, 100280.
- Adak, L., Kundu, D., Roy, K., Saha, M., & Roy, A. (2022). Reusable Iron/Iron Oxide-based Nanoparticles Catalyzed Organic Reactions. *Current Organic Chemistry*, 26(4), 399-417.
- Adesegun, S. A., Orabueze, C. I., & Coker, H. A. B. (2017). Antimalarial and Antioxidant Potentials of Extract and Fractions of Aerial part of *Borreria ocymoides* DC (Rubiaceae). *Pharmacognosy Journal*, 9(4).
- Amrillah, T., Notodidjojo, B. A., Kalimanjaro, M., Prastika, R. A., Nurrahman, A. M., Taufiq, A., ... & Setyawan, D. (2024). Crafting Iron Oxides for Next-Generation Biomedical Applications. *Crystal Growth & Design*.
- Aremu, S. O., Iheukwumere, C. C., Umeh, E. U., Olumuyiwa, E. O., & Fatoke, B. (2019). In-Vitro antimicrobial efficacy study of *Borreria verticillata* stem bark extracts against some dermatophytes and drug resistant pathogens. *Intl. J. Sci. Res Pub.* Research Gate. (accessed May 02, 2020). DOI, 10.
- Andrade, R. G., Veloso, S. R., & Castanheira, E. M. (2020). Shape anisotropic iron oxide-based magnetic nanoparticles: Synthesis and biomedical applications.

- International Journal of Molecular Sciences, 21(7), 2455.
- Alara, O. R., Ukaegbu, C. I., Abdurahman, N. H., Alara, J. A., & Ali, H. A. (2023). Plant-sourced antioxidants in human health: A state-of-art review. *Current Nutrition & Food Science*, 19(8), 817-830.
- Ali, L. M., Shaker, S. A., Pinol, R., Millan, A., Hanafy, M. Y., Helmy, M. H., & Mahmoud, S. A. (2020). Effect of superparamagnetic iron oxide nanoparticles on glucose homeostasis on type 2 diabetes experimental model. *Life sciences*, 245, 117361.
- Al-Saady, H. A. R. A., Ahmed, S. H., & Yousif, A. M. (2024). Synthesis of Green Iron Nanoparticles Using Henna Plant Extract for Seed Germination and Vegetative Growth of *Trigonella foenum-graecum*L, SAR J Med, 5 (1), 7-13. 7 SAR Journal of Medicine Abbreviated Key Title. SAR J Med.
- Antony, J., Meera, V., Raphael, V. P., & Vinod, P. (2024). Application of greenly synthesised zero-valent iron nanoparticles for iron removal from aqueous system. In IOP Conference Series: *Earth and Environmental Science* (Vol. 1326, No. 1, p. 012129). IOP Publishing.
- Awwad, A. M., Salem, N. M., Aqarbeh, M. M., & Abdulaziz, F. M. (2020). Green synthesis, characterization of silver sulfide nanoparticles and antibacterial activity evaluation. *Chem. Int*, 6(1), 42-48.
- Bibi, E., Hassan, S. M., Perveen, Z., Ali, B. S., Kanwal, M., Ibrahim, M. A., & Hassan, S. K. (2023). An Overview of Classification, Synthesis and Characterization of Nanomaterials. *Pakistan Journal of Science*, 75(04), 780-790.
- Boopathi, S., & Davim, J. P. (2023). Applications of Nanoparticles in Various Manufacturing Processes. In Sustainable Utilization of Nanoparticles and Nanofluids in Engineering Applications (pp. 1-31). IGI Global.
- Cheah, P., Brown, P., Qu, J., Tian, B., Patton, D. L., & Zhao, Y. (2021). Versatile surface functionalization of water-dispersible iron oxide nanoparticles with precisely controlled sizes. *Langmuir*, 37(3), 1279-1287.
- Conner, C. G., Veleva, A. N., Paunov, V. N., Stoyanov, S. D., & Velev, O. D. (2020). Scalable formation of concentrated monodisperse lignin nanoparticles by recirculation-enhanced flash nanoprecipitation. *Particle & Particle Systems Characterization*, 37(7), 2000122.
- Cheng, X., Jiang, X., Yin, S., Ji, L., Yan, Y., Li, G., ... & Sun, S. (2023). Instantaneous free radical scavenging by CeO2 nanoparticles adjacent to the Fe- N4 active sites for durable fuel cells. *Angewandte Chemie*, 135(34), e202306166.
- Drobot, M., Lungan, M. A., & Radu, I. (2022). FTIR Spectroscopy for Carbon Nanotube-Based Nanomaterials in Biomedical Applications. In Carbon Nanotubes for a Green Environment (pp. 233-256). Apple Academic Press.
- Dowlath, M. J. H., Musthafa, S. A., Khalith, S. M., Varjani, S., Karuppanan, S. K., Ramanujam, G. M., ... & Ravindran, B. (2021). Comparison of characteristics and biocompatibility of green synthesized iron oxide nanoparticles with chemical synthesized nanoparticles. *Environmental Research*, 201, 111585.
- Eaton, P., Quaresma, P., Soares, C., Neves, C., De Almeida, M. P., Pereira, E., & West, P. (2017). A direct comparison of

- experimental methods to measure dimensions of synthetic nanoparticles. *Ultramicroscopy*, 182, 179-190.
- Fam, Y., Sheppard, T. L., Diaz, A., Scherer, T., Holler, M., Wang, W., ... & Grunwaldt, J. D. (2018). Correlative Multiscale 3D Imaging of a Hierarchical Nanoporous Gold Catalyst by Electron, Ion and X-ray Nanotomography. *ChemCatChem*, 10(13), 2858-2867.
- Fierro-Aguirre, A., Gilón-Salazar, D. V., & Fontalvo, J. (2024). Synthesis of iron oxide nanoparticles with a ceramic membrane reactor: Effects on particles size distribution. *Chemical Engineering and Processing-Process Intensification*, 197, 109692.
- Filippov, S. K., Khusnutdinov, R., Murmiliuk, A., Inam, W., Zakharova, L. Y., Zhang, H., & Khutoryanskiy, V. V. (2023). Dynamic light scattering and transmission electron microscopy in drug delivery: a roadmap for correct characterization of nanoparticles and interpretation of results. *Materials Horizons*, 10(12), 5354-5370.
- Gui, S., Tang, W., Huang, Z., Wang, X., Gui, S., Gao, X., ... & Wang, X. (2023). Ultrasmall Coordination Polymer Nanodots Fe-Quer Nanozymes for Preventing and Delaying the Development and Progression of Diabetic Retinopathy. *Advanced Functional Materials*, 33(36), 2300261.
- Hala, A. A., Ahmed, I. H., Mohamed, M. H., & Ahmed, T. E. A. (2022). Biosynthesis of iron nanoparticles by petroleum degrading bacteria and evaluation of their potential for removal of petroleum contaminants. *Journal of Environmental Science*, 51(5), 33-70.
- Haider, F. U., Zulfiqar, U., ul Ain, N., Hussain, S., Maqsood, M. F., Ejaz, M., ... & Li, Y. (2024). Harnessing plant extracts for eco-friendly synthesis of iron nanoparticle (Fe-NPs): Characterization and their potential applications for ameliorating environmental pollutants. *Ecotoxicology and Environmental Safety*, 281, 116620.
- Izuogu, N. B., Bello, O. E., & Bello, O. M. (2020). A review on *Borreria verticillata*: A potential bionematicide, channeling its significant antimicrobial activity against root-knot nematodes. *Heliyon*, 6(10).
- Irgibaeva, I., Barashkov, N., Sakhno, T., Mantel, A., Mendigaliyeva, S., Barashkova, I., & Sakhno, Y. (2020). Synthesis of iron nanoparticles by thermal decomposition of diironnonacarbonyl in ionic liquid and their potential use as nanotracers for mixer studies in liquids feeds. *Advances in Chemical Engineering and Science*, 10(3), 201-209.
- Jamzad, M., & Kamari B. M. (2020). Green synthesis of iron oxide nanoparticles by the aqueous extract of *Laurus nobilis* L. leaves and evaluation of the antimicrobial activity. *Journal of nanostructure in Chemistry*, 10(3), 193-201.
- Jideani, A. I., Silungwe, H., Takalani, T., Omolola, A. O., Udeh, H. O., & Anyasi, T. A. (2021). Antioxidant-rich natural fruit and vegetable products and human health. *International Journal of Food Properties*, 24(1), 41-67.
- Kamanna, K., & Amaregouda, Y. (2023). Water Mediated Green Method Synthesis of Bioactive Heterocyclic Reported Between 2012-2021 Accelerated by Microwave Irradiation: A Decennary Update. *Current Organocatalysis*, 10(3), 160-179.
- Khan, Y., Sadia, H., Ali Shah, S. Z., Khan, M. N., Shah, A. A., Ullah, N., & Khan, M. I. (2022). Classification, synthetic, and

- characterization approaches to nanoparticles, and their applications in various fields of nanotechnology: A review. *Catalysts*, 12(11), 1386.
- Kandoor, S., Dhar, S., Kumar, L., Arackal, S., Sai, R., & Kamanna, K., & Amaregouda, Y. (2023). Water Mediated Green Method Synthesis of Bioactive Heterocyclic Reported Between 2012-2021 Accelerated by Microwave Irradiation: A Decennary Update. *Current Organocatalysis*, 10(3), 160-179.
- Kumar, R., Kumari, N., & Sahoo, G. C. (2024). Iron Oxide-Based Nanoparticles in Modern Antimicrobial and Antiviral Applications. In *Nanoparticles in Modern Antimicrobial and Antiviral Applications* (pp. 289-303). Cham: Springer International Publishing.
- Kunjan, F., Shanmugam, R., & Govindharaj, S. (2024). Evaluation of Free Radical Scavenging and Antimicrobial Activity of *Coleus amboinicus*-Mediated Iron Oxide Nanoparticles. *Cureus*, 16(3).
- Kotresh, M. G., Patil, M. K., & Inamdar, S. R. (2021). Reaction temperature based synthesis of ZnO nanoparticles using co-precipitation method: Detailed structural and optical characterization. *Optik*, 243, 167506.
- Kontagora, G. F., Lawal, N., Adebote, D. A., Kamba, B., Nafiu, M. I., & Jufare, A. I. (2020). Some preliminary phytochemical screening and assessment of four solvents extracts of button weed (*Borreria verticillata*). *Journal of Applied Sciences and Environmental Management*, 24(12), 2085-2088.
- Lu, Z., Yu, D., Nie, F., Wang, Y., & Chong, Y. (2023). Iron Nanoparticles Open Up New Directions for Promoting Healing in Chronic Wounds in the Context of Bacterial Infection. *Pharmaceutics*, 15(9), 2327.
- Mohil, R., & Kaushik, N. (2024). Overview on Nanoparticle Classes, Design and Perspectives.
- Maniah, K. (2024). Antifungal, antioxidant, and photocatalytic activities of greenly synthesized iron oxide nanoparticles. *Open Chemistry*, 22(1), 20240031.
- , K., Saha, A., Bhattacharjee, S., Mallick, A., & Sarkar, B. (2022). Nanoscale iron for sustainable aquaculture and beyond. *Biocatalysis and Agricultural Biotechnology*, 44, 102440.
- Miguel, L. M., Sobrado, S. V., Janssens, S., Dessein, S., & Cabral, E. L. (2018). The monotypic Brazilian genus *Diacrodon* is a synonym of *Borreria* (*Spermacoceae*, *Rubiaceae*): Morphological and molecular evidences. *Anais da Academia Brasileira de Ciências*, 90(02), 1397-1415.
- Namasivayam, S. K. R. (2024). Eco friendly, green route method for the preparation of poly ethylene glycol (PEG) mediated surface modified iron oxide nanoparticles (PEG-IONps) with potential biological activities. *Environmental Quality Management*.
- Nemati, Z., Alonso, J., Rodrigo, I., Das, R., Garaio, E., García, J. Á., ... & Srikanth, H. (2018). Improving the heating efficiency of iron oxide nanoparticles by tuning their shape and size. *The Journal of Physical Chemistry C*, 122(4), 2367-2381.
- Nekvapil, F., Bortnic, R. A., Leoştean, C., Barbu-Tudoran, L., & Bunge, A. (2022). Characterization of the lattice transitions and impurities in manganese and zinc doped ferrite nanoparticles by Raman spectroscopy and x-ray diffraction (XRD). *Analytical Letters*, 56(1), 42-52.

- Panda, K. C., Varaha Bera, R. K. V., Sahoo, B. M., & Swain, P. (2023). Green Chemistry Approach for the Synthesis of Isoxazole Derivatives and Evaluation of their Anti-epileptic Activity. *Current Drug Discovery Technologies*, 20(3), 74-81.
- Panneerselvam, C., Alshehri, M. A., Saif, A., Faridi, U., Khasim, S., Mohammed Saleh, Z. M., ... & Al-Aoh, H. A. (2024). Green synthesis of Abutilon indicum (L) derived iron oxide (FeO) nanoparticles with excellent biological, anticancer and photocatalytic activities. *Polyhedron*, 257, 117022.
- Patreanu, I., Niculescu, V. C., Enache, S., Iacob, C., & Teodorescu, M. (2023). Structural characterization of silica and amino-silica nanoparticles by Fourier transform infrared (FTIR) and raman spectroscopy. *Analytical Letters*, 56(2), 390-403.
- Pathak, J., Singh, D. K., Singh, P. R., Kumari, N., Jaiswal, J., Gupta, A., & Sinha, R. P. (2024). Application of nanoparticles in agriculture: nano-based fertilizers, pesticides, herbicides, and nanobiosensors. In *Molecular Impacts of Nanoparticles on Plants and Algae* (pp. 305-331). Academic Press.
- Plakas, K. V., Mantza, A., Sklari, S. D., Zaspalis, V. T., & Karabelas, A. J. (2019). Heterogeneous Fenton-like oxidation of pharmaceutical diclofenac by a catalytic iron-oxide ceramic microfiltration membrane. *Chemical Engineering Journal*, 373, 700-708.
- Ramirez, O., Ramasamy, P., Chan Choi, Y., & Lee, J. S. (2018). Morphology transformation of chalcogenide nanoparticles triggered by cation exchange reactions. *Chemistry of Materials*, 31(1), 268-276.
- Ridolfo, R., Tavakoli, S., Junnuthula, V., Williams, D. S., Urtti, A., & van Hest, J. C. (2020). Exploring the impact of morphology on the properties of biodegradable nanoparticles and their diffusion in complex biological medium. *Biomacromolecules*, 22(1), 126-133.
- Rauf, A., Ibrahim, M., Ahmad, Z., Muhammad, N., Al-Awthman, Y. S., Bahattab, O. S., ... & Thiruvengadam, M. (2024). Green synthesis, characterization, and biomedical applications of Iron nanoparticles synthesized from the alcoholic extract of the aerial part of *Micromeria biflora* (Buch. Ham. ex D. Don) Benth.
- Sala, M., Diab, R., Elaissari, A., & Fessi, H. (2018). Lipid nanocarriers as skin drug delivery systems: Properties, mechanisms of skin interactions and medical applications. *International journal of pharmaceutics*, 535(1-2), 1-17.
- Samrot, A. V., Ram Singh, S. P., Deenadhayalan, R., Rajesh, V. V., Padmanaban, S., & Radhakrishnan, K. (2022). Nanoparticles, a double-edged sword with oxidant as well as antioxidant properties—A review. *Oxygen*, 2(4), 591-604.
- Shaikh, K. R., Pawar, A. R., Salmote, A. D., Shinde, S. A., & Undre, P. B. (2024). Exploring the effect of crystalline phase on photocatalytic, antimicrobial and antioxidant performance of magnetic iron oxide nanoparticles. *Nano-Structures & Nano-Objects*, 38, 101166.
- Shanmugam, R., Tharani, M., Abullais, S. S., Patil, S. R., & Karobari, M. I. (2024). Black seed assisted synthesis, characterization, free radical scavenging, antimicrobial and anti-inflammatory activity of iron oxide

- nanoparticles. *BMC Complementary Medicine and Therapies*, 24(1), 241.
- Sharma, P., Singh, A., & Kumar, R. (2023). Green synthesis of silver nanoparticles using *Borreria verticillata* and their enhanced bioactivity against diabetes and oxidative stress. *Materials Science and Engineering: C*, 143, 112133. <https://doi.org/10.1016/j.msec.2023.112133>
- Sheth, M., & Apte, S. (2023). Review of synthesis and applications of Iron oxide nanoparticles. *The Bombay Technologist*.
- Scurti, S., Caretti, D., Mollica, F., Di Antonio, E., & Amorati, R. (2022). Chain-breaking antioxidant and peroxyl radical trapping activity of phenol-coated magnetic iron oxide nanoparticles. *Antioxidants*, 11(6), 1163.
- Tangara, D., Diop, A., Tirera, H., Koumare, B. Y., Naco, M. E. B., Fall, D., ... & Diop, Y. M. (2022). *Borreria verticillata* plante médicinale sénégalaise: Étude de l'activité antioxydante d'extraits méthanoliques, chloroformiques, aqueux et acétates de la plante entière (racine, tige, feuille, fleurs). *Journal of Applied Biosciences*, 171(1), 17812-17820.
- Tareq, A. M., Farhad, S., & Chakraborty, S. (2019). Experimental analysis of isolated compounds of *Borreria hispida* (L) in the context of antioxidant. *Discovery Phytomedicine*, 6(3), 138-142.
- Tripathi, S., Mahra, S., Tiwari, K., Rana, S., Tripathi, D. K., Sharma, S., & Sahi, S. (2023). Recent advances and perspectives of nanomaterials in agricultural management and associated environmental risk: a review. *Nanomaterials*, 13(10), 1604.
- Tsilo, P. H., Basson, A. K., Ntombela, Z. G., Dlamini, N. G., & Pullabhotla, R. V. (2023). Application of Iron Nanoparticles Synthesized from a Biofloculant Produced by Yeast Strain *Pichia kudriavzevii* Obtained from Kombucha Tea SCOBY in the Treatment of Wastewater. *International Journal of Molecular Sciences*, 24(19), 14731.
- Turrina, C., Schoenen, M., Milani, D., Klassen, A., González, D. M. R., Cvirn, G., ... & Schwaminger, S. P. (2023). Application of magnetic iron oxide nanoparticles: thrombotic activity, imaging and cytocompatibility of silica-coated and carboxymethyl dextrane-coated particles. *Colloids and Surfaces B: Biointerfaces*, 228, 113428.
- Velayudham, R., & Natarajan, J. (2024). Multifunctional application of different iron oxide nanoparticles. *Zeitschrift für Physikalische Chemie*, (0).
- Vera-Reyes, I., Vázquez-Núñez, E., Lira-Saldivar, R. H., & Méndez-Argüello, B. (2018). Effects of nanoparticles on germination, growth, and plant crop development. *Agricultural Nanobiotechnology: Modern Agriculture for a Sustainable Future*, 77-110.
- Vyas, R., Mathur, M., Singh, A., & Mathur, N. (2024). Mycofabrication of Iron Nanoparticles: Applications and Future Prospectus. *Nanofabrication*, 9.
- Wu, A., Zhao, W., & Hao, B. (2021). Fluorescent and magnetic nanocomposites of Y_2O_3 : Eu^{3+} , Dy^{3+} and Fe or Fe_3O_4 . *Journal of Nanoparticle Research*, 23(1), 14.
- Yamazaki, Y., Shirai, N., Nakagawa, Y., Uchida, S., & Tochikubo, F. (2018). Chemical reaction process for magnetite nanoparticle synthesis by atmospheric-pressure DC glow-discharge

- electrolysis. Japanese Journal of Applied Physics, 57(9), 096203.
- Yang, L., Yan, Z., Yang, L., Yang, J., Jin, M., Xing, X., ... & Shui, L. (2020). Photothermal conversion of SiO₂@Au nanoparticles mediated by surface morphology of gold cluster layer. RSC advances, 10(55), 33119-33128.
- Ying, S., Guan, Z., Ofoegbu, P. C., Clubb, P., Rico, C., He, F., & Hong, J. (2022). Green synthesis of nanoparticles: Current developments and limitations. *Environmental Technology & Innovation*, 26, 102336.
- Zafar, S., Faisal, S., Jan, H., Ullah, R., Rizwan, M., Abdullah, ... & Khattak, A. (2022). Development of iron nanoparticles (FeNPs) using biomass of enterobacter: Its characterization, antimicrobial, anti-Alzheimer's, and enzyme inhibition potential. *Micromachines*, 13(8), 1259.
- Zakharov, Y. A., Popova, A. N., Pugachev, V. M., Zakharov, N. S., Tikhonova, I. N., Russakov, D. M., ... & Sadykova, L. R. (2023). Morphology and Phase Compositions of FePt and CoPt Nanoparticles Enriched with Noble Metal. *Materials*, 16(23), 7312.
- Zhang, X., Suo, H., Zhang, Z., Ye, S., Ma, L., Liu, M., ... & Wang, Q. (2022). Two-dimensional X-ray diffraction characterization of growth mechanism of double perovskite-structured nanoparticles in thin films prepared via metal-organic decomposition. *CrystEngComm*, 24(21), 3913-3920.
- Zhou, Y., Liu, C., Yu, Y., Yin, M., Sun, J., Huang, J., & Song, H. (2020). An organelle-specific nanozyme for diabetes care in genetically or diet-induced models. *Advanced Materials*, 32(45), 2003708.
- Kumar S. S. (2019)., "Green synthesis and characterization of iron nanoparticles using plant extracts," *Journal of Materials Chemistry*, vol. 10, pp. 200-210.

Appendix I:

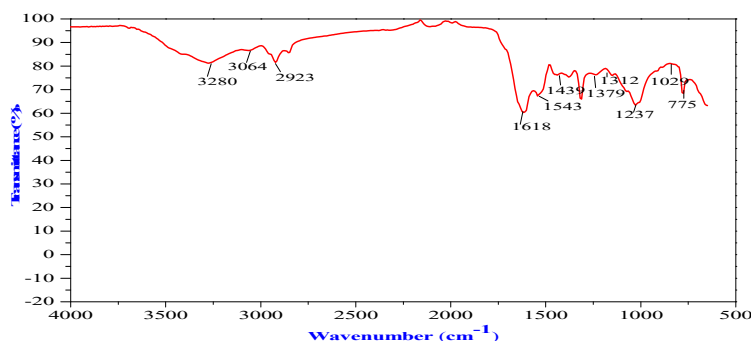


Figure 1: FT-IR spectrum of *Borreria verticillata* Extract

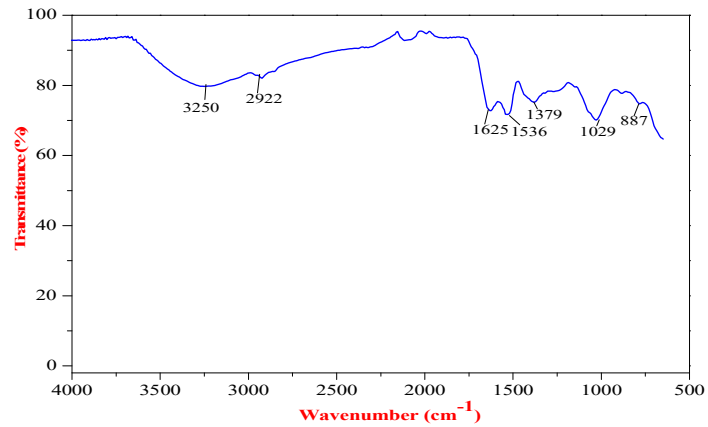


Figure 2: FT-IR spectrum of *Borreria verticillata* FeNPs

Appendix II:

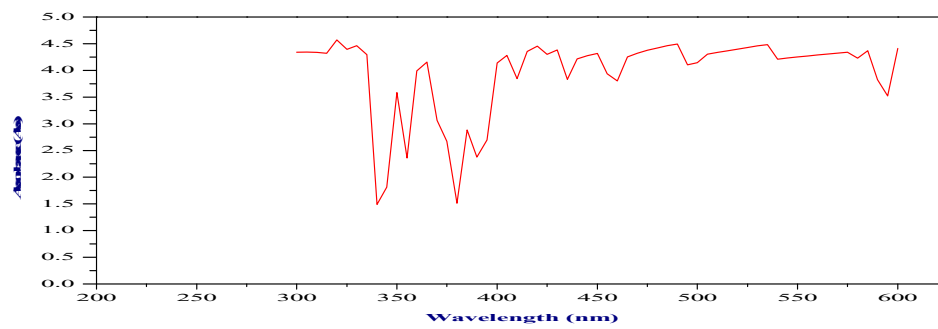


Figure 3: UV-Vis spectrum of *Borreria verticillata* Extract

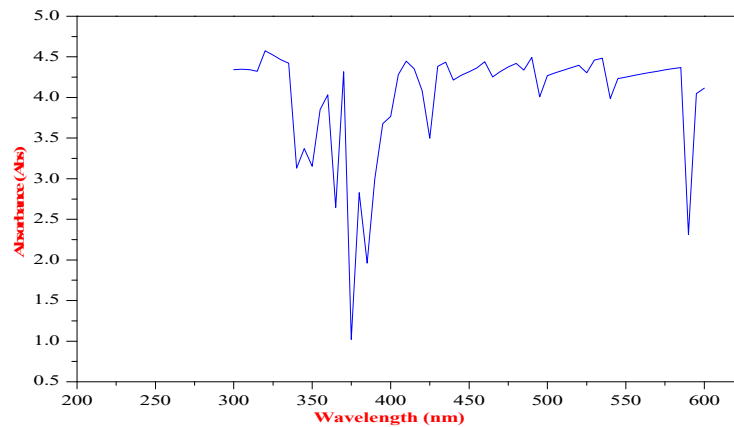


Figure 4: UV-Vis Spectrum of *Borreria Verticillata* FeNPs.

Appendix III:

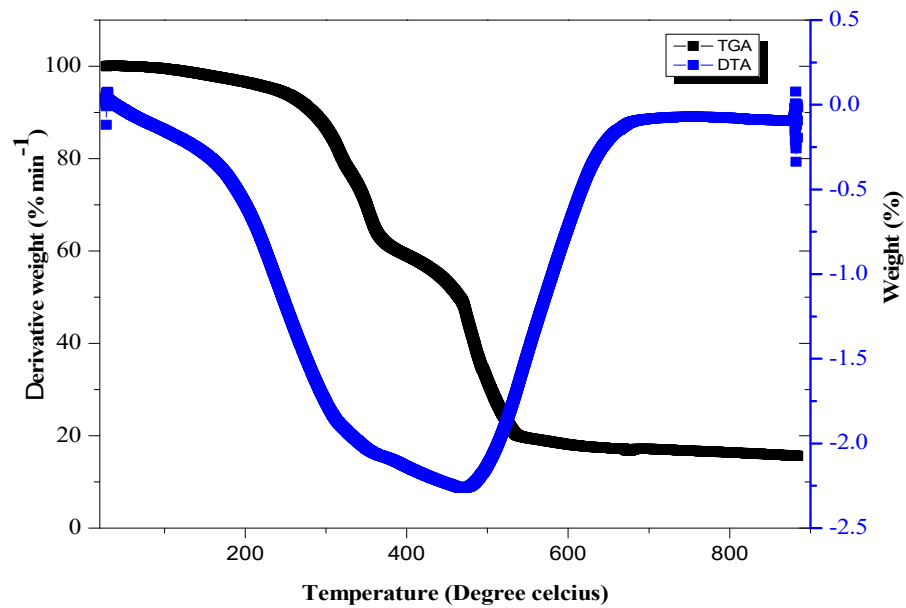


Figure 4: TG-DTA thermogram (curve) of *Borreria verticillata* Extract

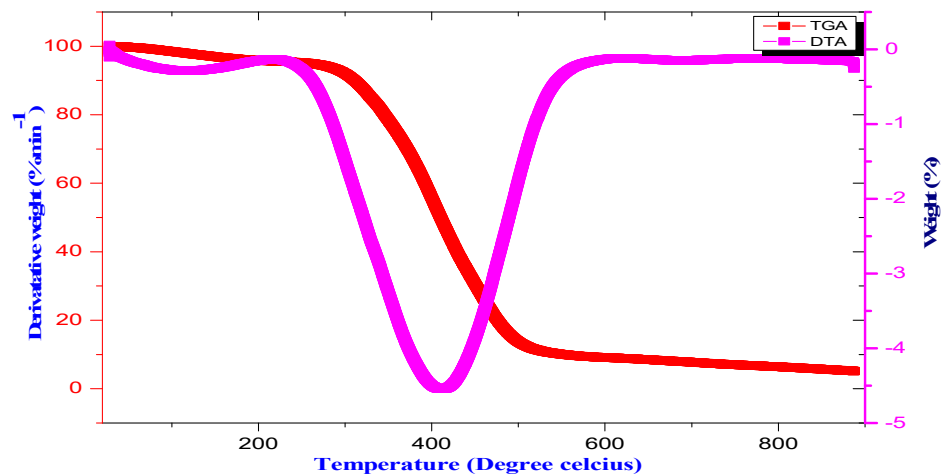


Figure 6: TG-DTA Curve of *Borreria verticillata* Fe Nanoparticles

Appendix IV:

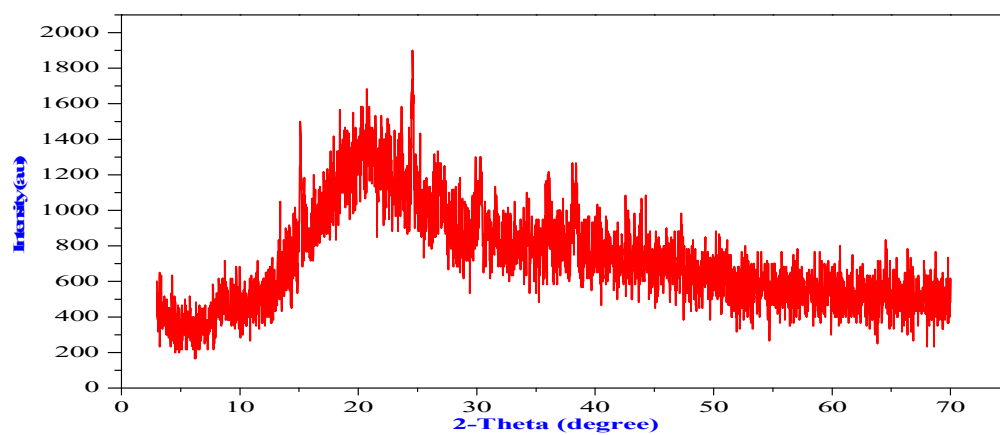


Figure 7: XRD Spectrum of *Borreria verticillata* Extract

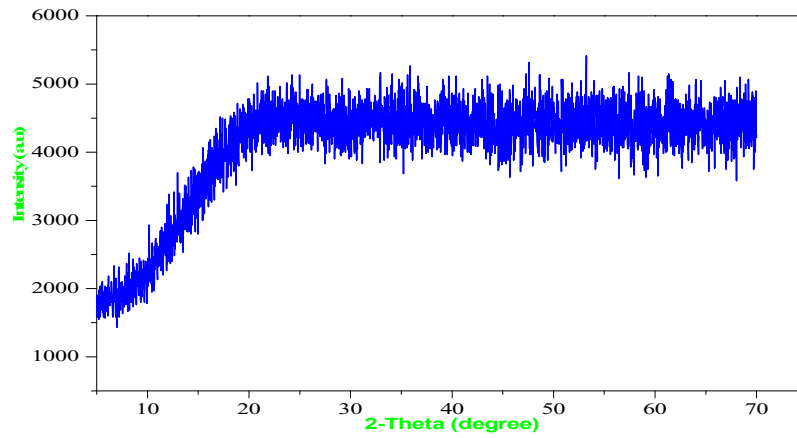


Figure 8: XRD spectrum of *Borreria verticillata* Iron Nanoparticles